Technology for a large-area reflection grating spectrometer on Constellation-X

S.M. Kahn, F. Paerels, A. Rasmussen - Columbia Univ.
M.L. Schattenburg, G.R. Ricker, M.W. Bautz, J.P. Doty, G.Y. Prigozhin - MIT
J. Nousek, D. Burrows, J.E. Hill - Penn State Univ.
W. Cash - Univ. of Colorado

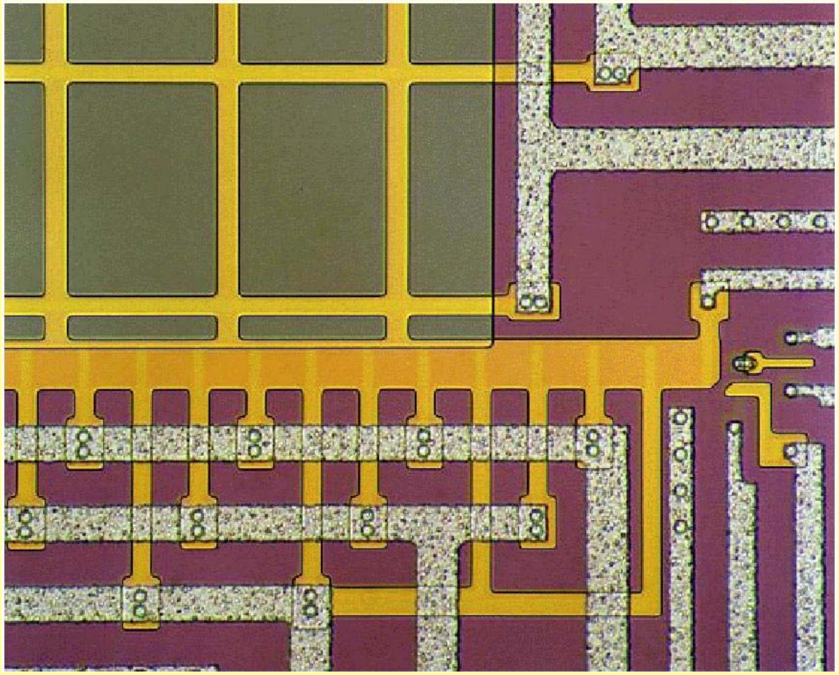

Resistive Gate CCD (electron micrograph)

Anisotropically etched Si grating with (111) plane facets

The Role of a Reflection Grating Spectrometer on Constellation-X

- The soft X-ray band is rich in spectral features: (K-shell of C, N, O, Ne, Mg, Si, S; L-shell of Fe, Ni). $\lambda/\Delta\lambda > 300$ required for unambiguous line identifications and other plasma diagnostics.

- For microcalorimeters, ΔE is constant. Thus $\lambda/\Delta\lambda$ falls linearly with energy and is insufficient at energies less than ~ 0.5 keV. In addition, the microcalorimeter efficiency is limited at low energies due to the incorporation of long wavelength blocking filters.

- For a dispersive spectrometer, $\Delta\lambda$ is approximately constant, so $\lambda/\Delta\lambda$ rises inversely with decreasing energy. For reflection gratings, the efficiency also increases at low energies due to increasing reflection efficiency. This is especially important for spectroscopy of sources at cosmological distances where key spectral diagnostics are redshifted down to low energies!

Design considerations - what λ range?

(courtesy Frits Paerels)

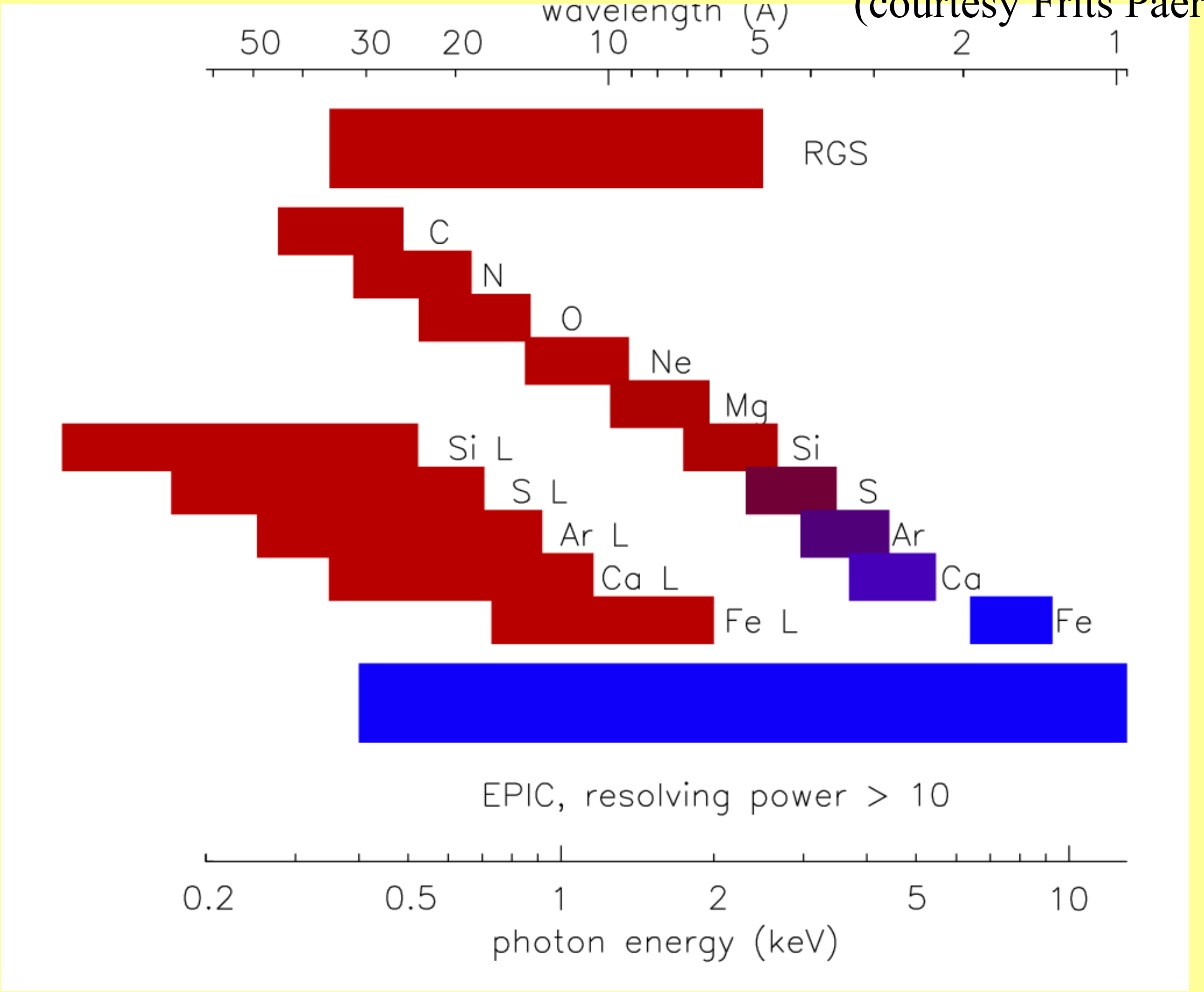

Design considerations - what $\lambda/\Delta\lambda$ is required?

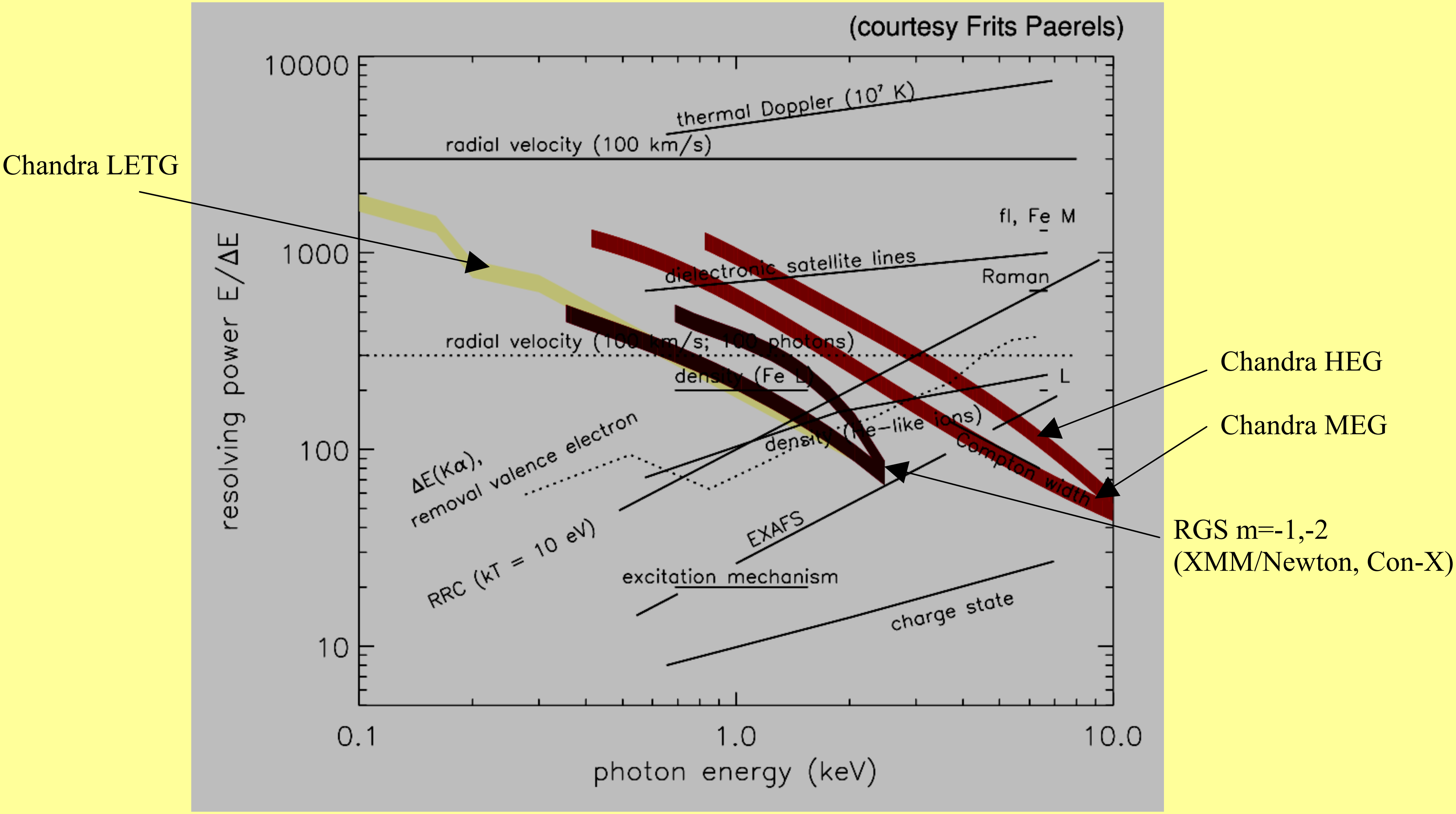

Baseline Design: Diffraction Geometry

Dispersion Equation:

$$\cos\beta = \cos\alpha + \frac{m\lambda}{d}$$

Blaze Condition:

$$\alpha + \delta = \beta_{\rm B} - \delta = \gamma$$

$$m\lambda_{\rm B} = 2d\sin\gamma\sin\delta$$

Resolving Power at Blaze:

$$R_{\rm B} = \frac{\gamma}{\Delta\theta}\left(\frac{1}{\eta} - 1\right)$$

$$\eta \equiv \frac{\sin\alpha}{\sin\beta_{\rm B}}$$

Optimization:

$$\mathit{Effic}_{\rm B} = \eta^2 \mathit{Refl}\,(\gamma, \lambda_{\rm B})$$

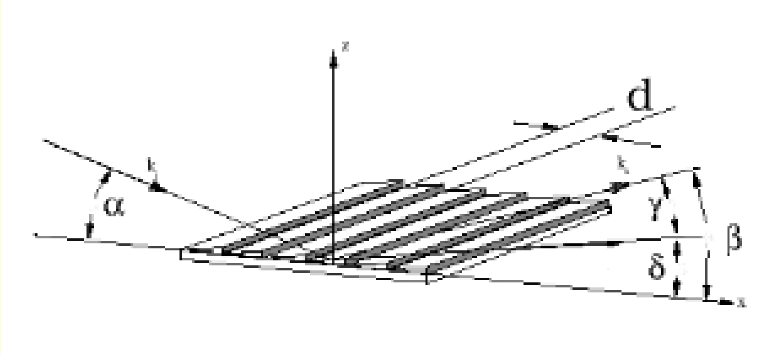

Optimized Parameters:

R_B	=	400	
λ_B	=	20	Angstroms
d	=	24,547	Angstroms
δ	=	0.605	degrees
γ	=	2.21	degrees
α	=	1.61	degrees
η	=	0.57	

Baseline Design: Inverted Rowland Circle

- Essentially aberration free at all wavelengths.
- Design is compact - no additional length required behind the focus.
- Gratings require varied line spacing.
- Only cover outer half of the mirror shells at ~57% throughput. Non-intercepted light goes to the microcalorimeter at the telescope focus.

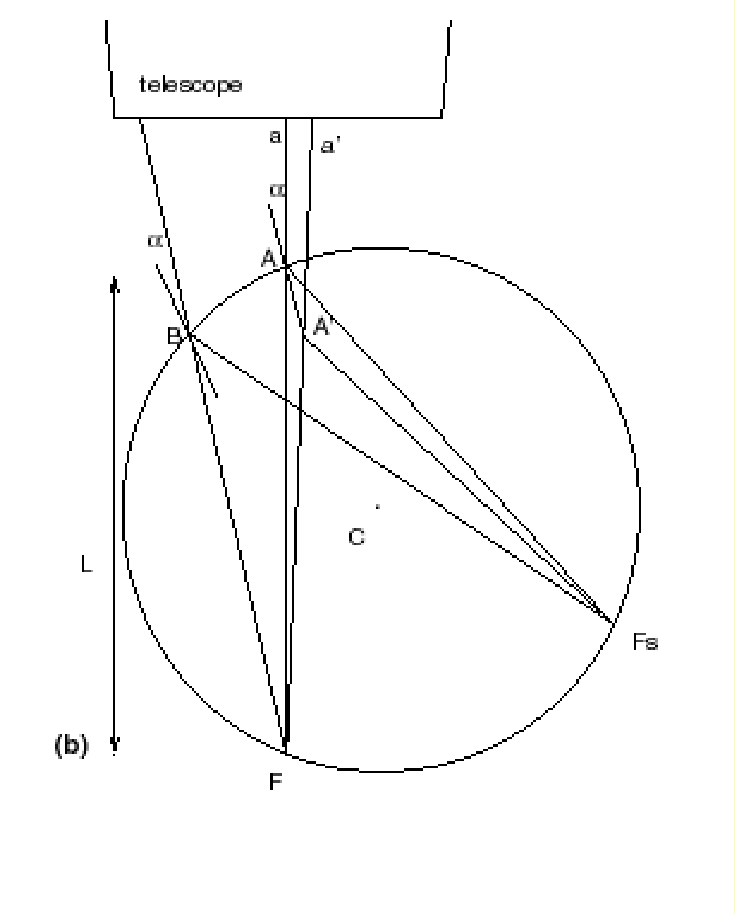

Baseline Design: Scientific Performance

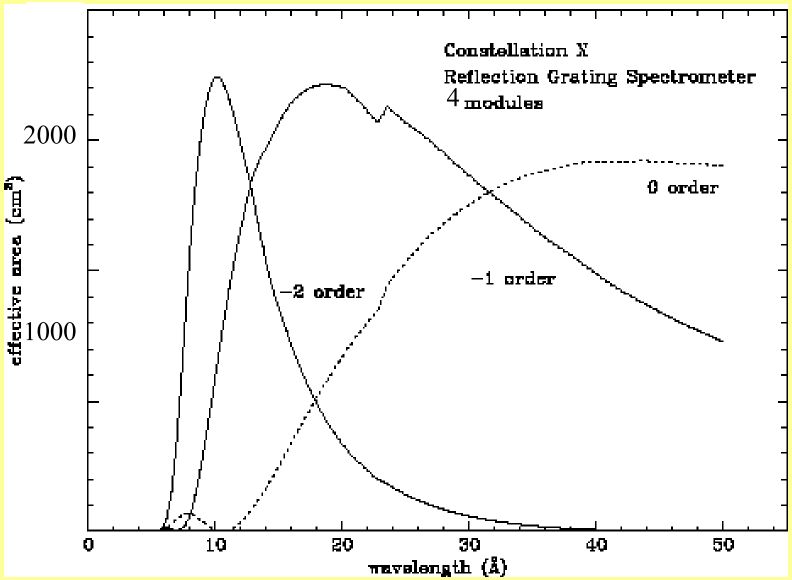

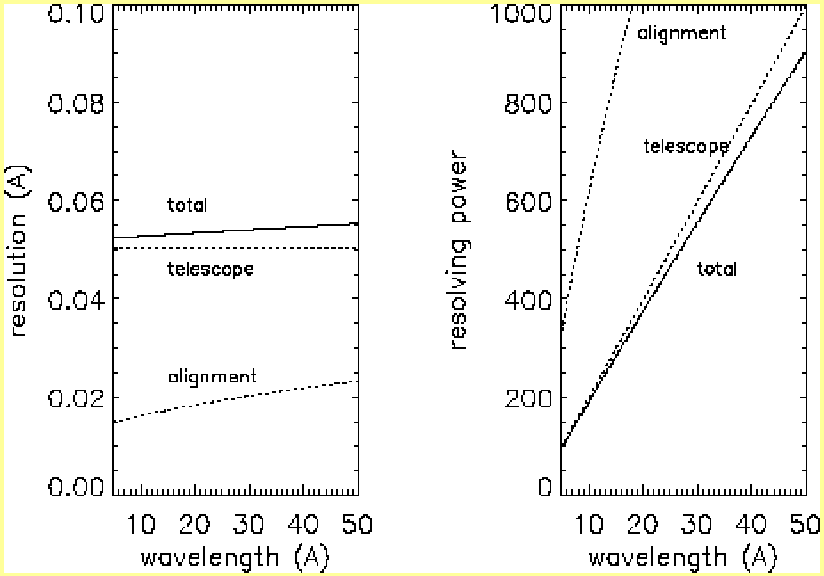

Left: Theoretical effective area functions for a grating array intercepting the outer half of the SXTs. Gratings are gold coated, with smooth triangular groove and parameters described on the previous page. Right: Resolving power function for m=-1 and nominal (2") grating flatness and 2" alignment budgets.

Fabrication Approach: Reflection Grating Array

- For *XMM*, the gratings were epoxy replicated onto precision machined SiC substrates. This approach is too costly, time consuming, and **heavy** for Constellation-X.
- Instead, we propose to fabricate the gratings directly using interference lithography on graze-cut silicon wafers.
- Very thin (< 100 micron) grating **membranes** are produced using buried oxide silicon wafers. These are then mounted under uniform tension onto flat, lightweighted frames.
- The primary distortion is **twist**, which is removed by positioning the frames against four coplanar bosses, precision machined on alignment rails mounted to the structure.
- The integrating structure will consist of two concentric cylinders connected by a web that supports the rails. This will be integrally mounted to the telescope spider at the exit plane of the telescope.

Grating Fabrication: Possible Modular Mounting Scheme

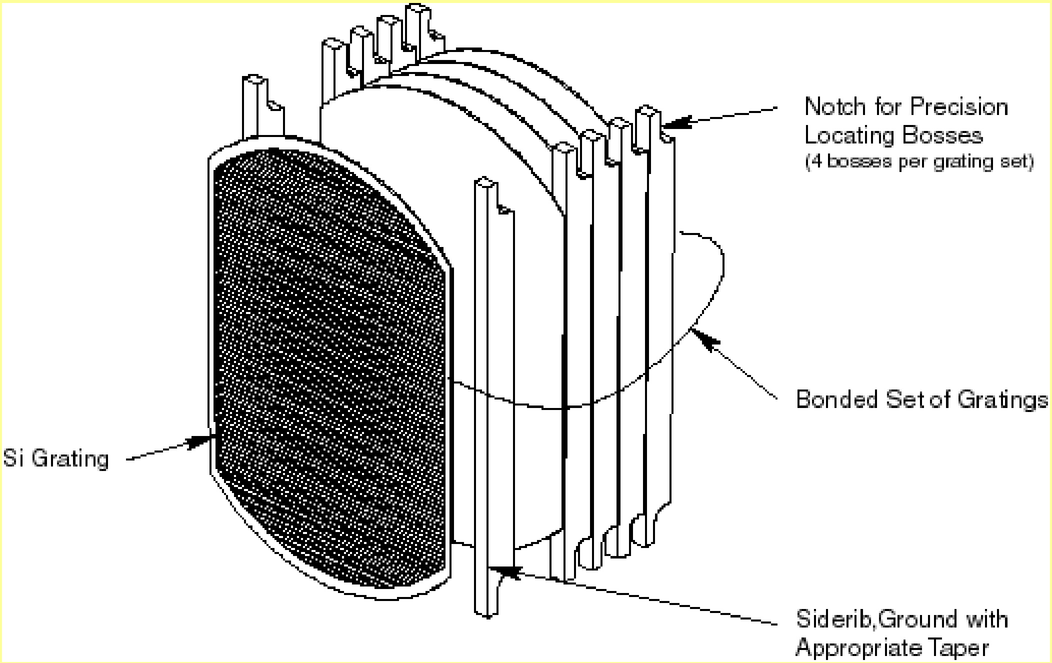

Possible approach to assembling and mounting gratings into sub-modules. The thin silicon gratings are bonded to precision ground sideribs with the correct taper to stack the gratings at the appropriate angles and separations. The ribs are notched for precision locating against reference bosses in the full-up assembly.

Grating Fabrication: Integrating Structure Concept

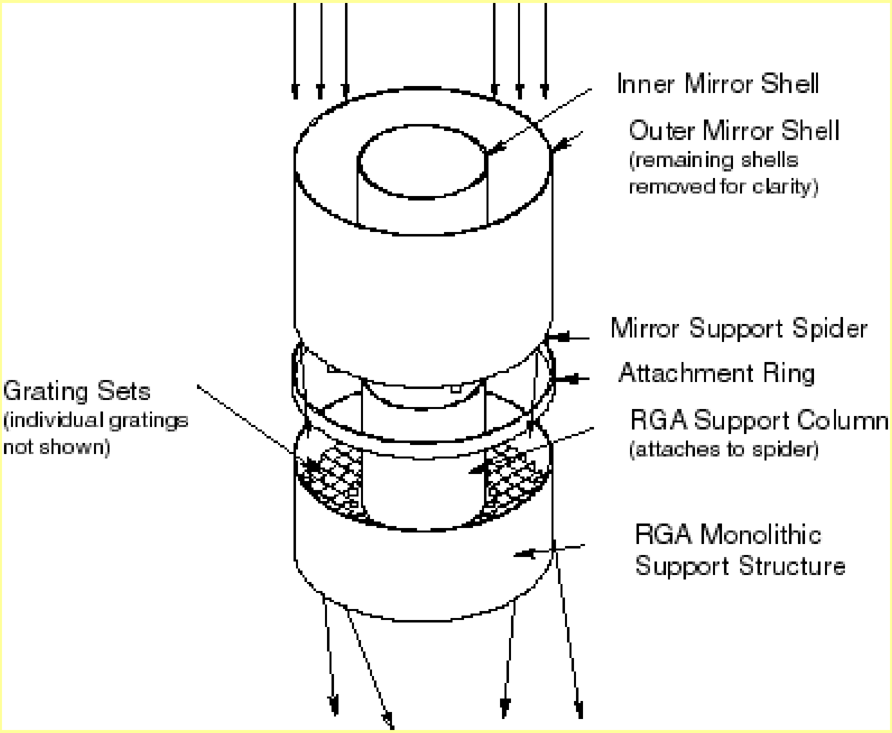

A sketch of a possible design for the integrating structure that supports the reflection grating array at the exit plane of the telescope. The mirror support spider and attachment ring might also be integral to the monolithic RGA support structure.

Classic In-Plane Mount

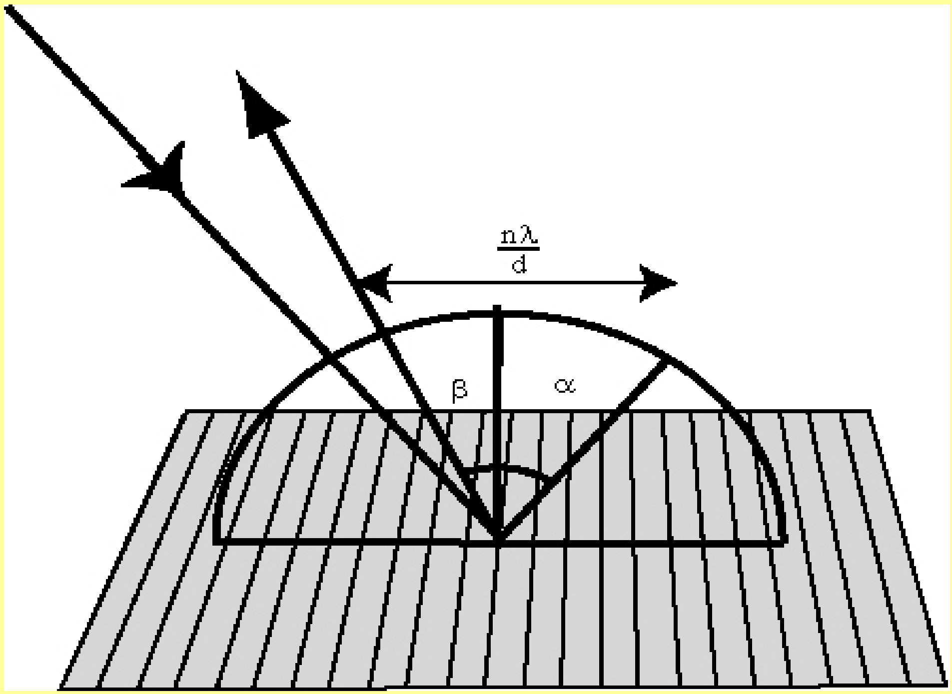

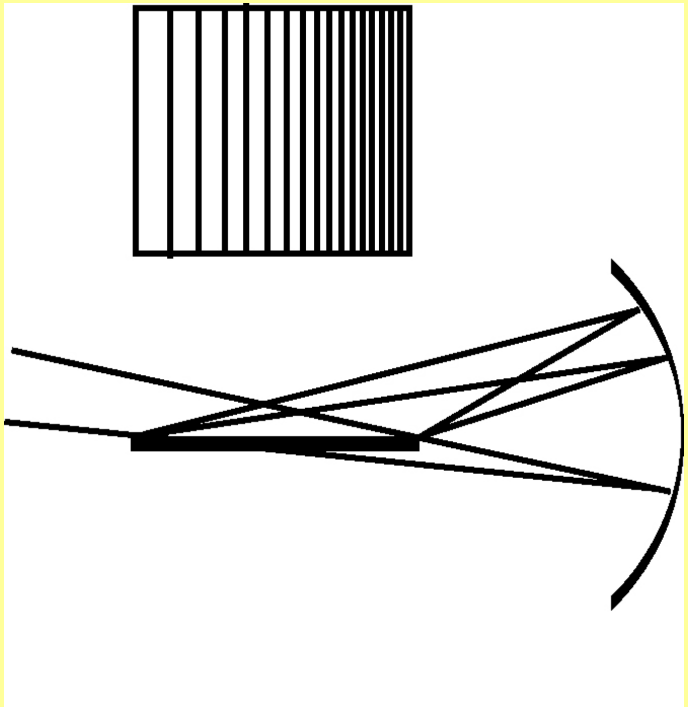

The Off-plane Mount

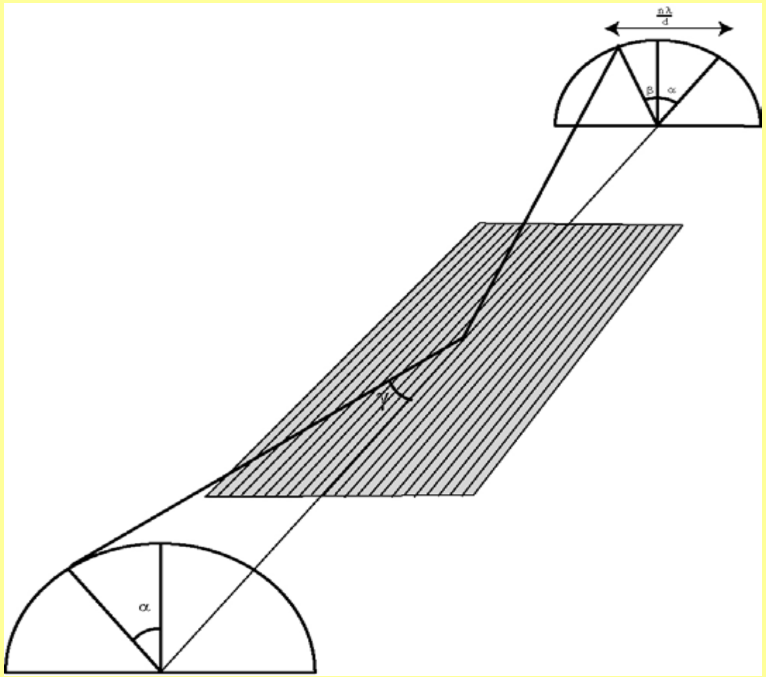

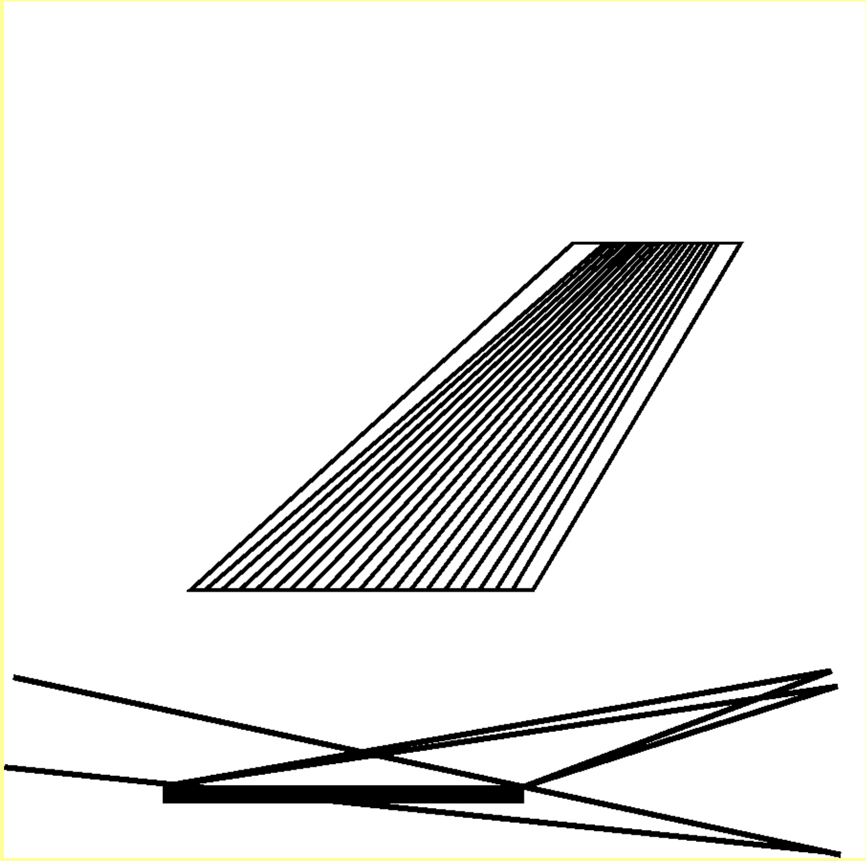

An Off-plane X-ray Spectrum

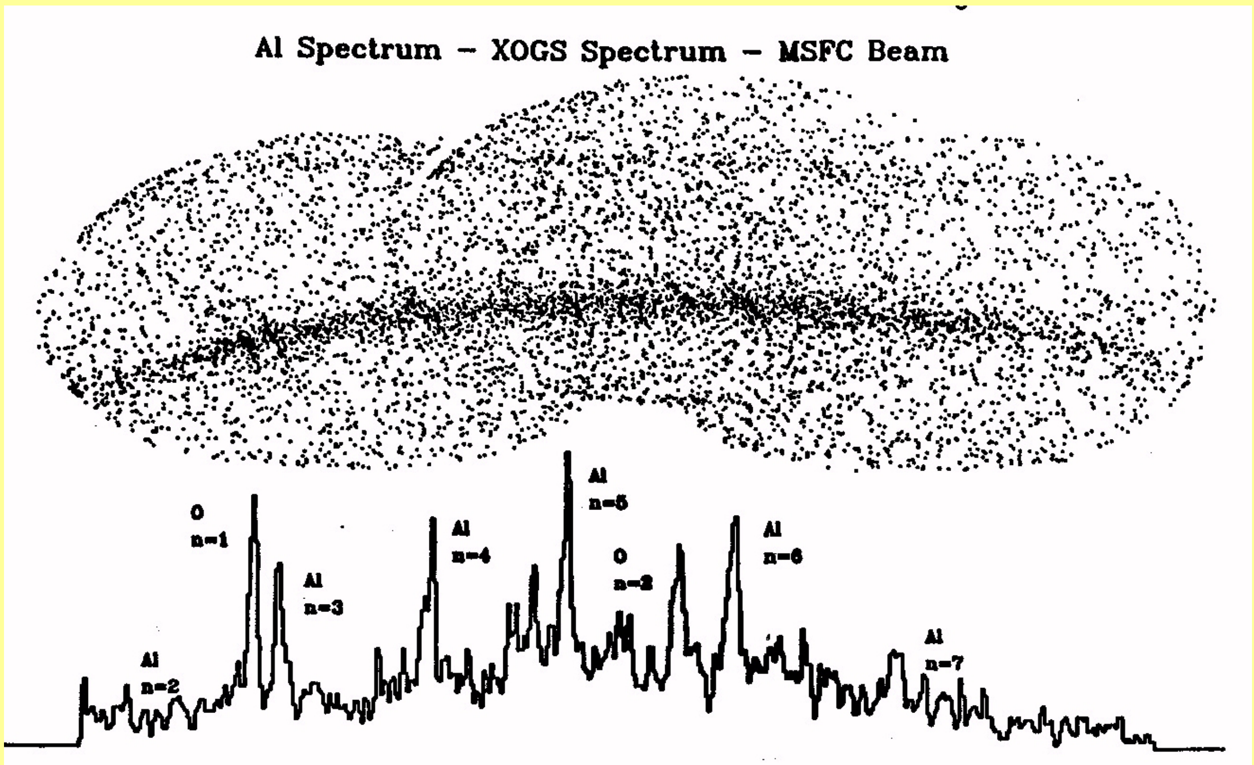

Spectrum from Al target shows Al kα (λ=8.3A, E=1.4keV) in orders n=2 though n=7. Contamination from O kα (λ=23.6A, E=0.525keV) is also clearly present in first and second orders. Note that the blaze function is about 20 deg. in azimuthal angle. This spectrum was obtained by the XOGS spectrograph in the beam facility at Marshall Space Flight Center using a 3600 g/mm grating array in the off-plane mount. The signal in the sum of orders 3 through 6 is about 40% of the incident signal. With a CCD these orders can be recombined without loss of signal or resolution.

Off-plane Tradeoffs

PRO

- Higher Throughput
- Higher Resolution
- Better Packing Geometry
- Looser Alignment Tolerances

CON

- Higher Groove Density

Packing Geometry

In-plane

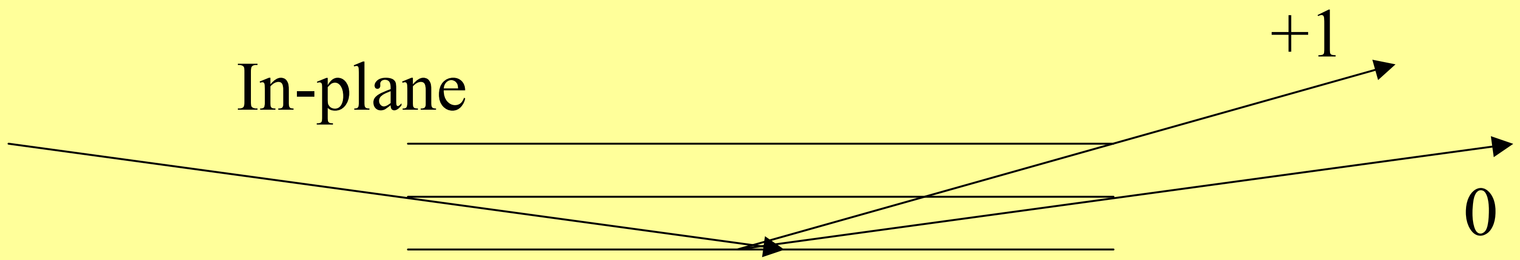

Central grating must be removed.
Half the light goes through.

Off-plane

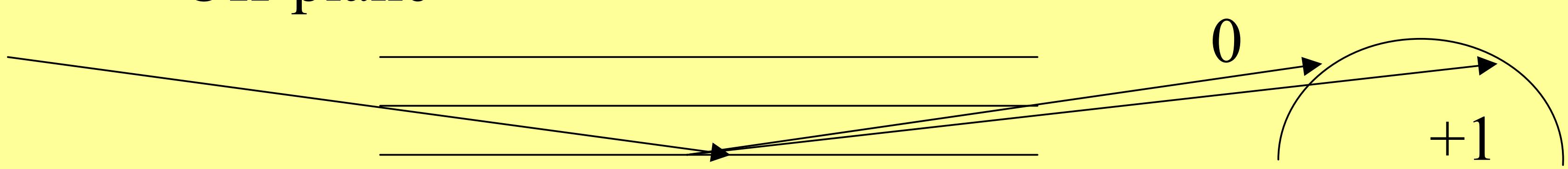

Gratings may be packed optimally

Throughput

- Better Groove Illumination
- Fewer available orders
- Constant Graze Angle

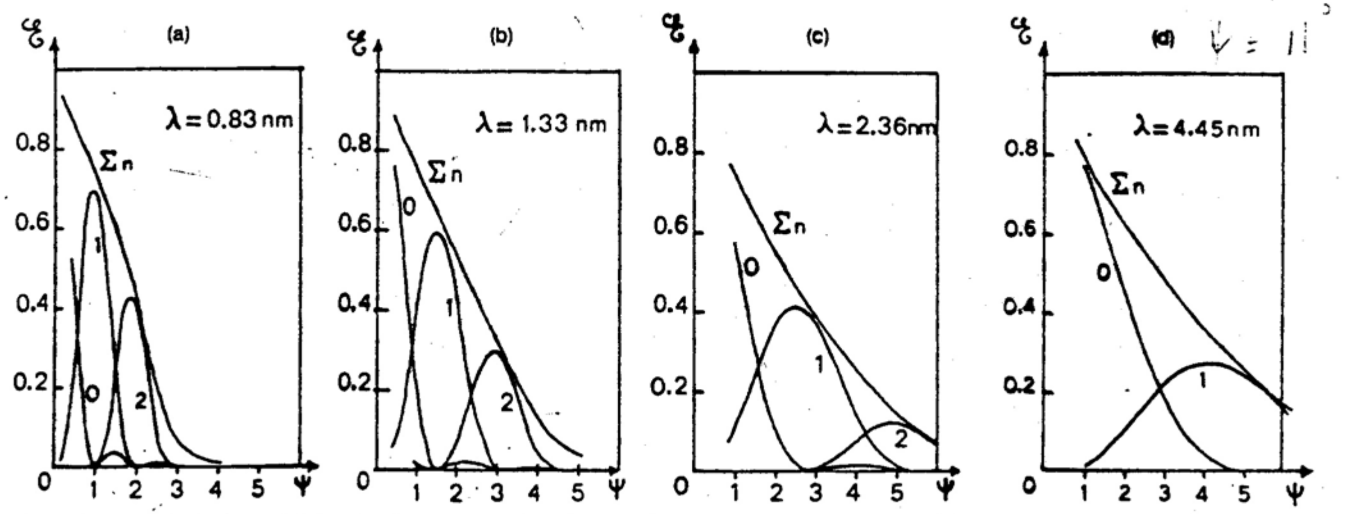

Fig. 1. Theoretical absolute efficiencies for a 3600-grooves/mm, 5° blaze angle, 90° apex angle gold grating as a function of the grazing angle ψ, for an extreme off-plane mounting and four different wavelengths. The incident wave vector lies in a plane parallel to the grooves and perpendicular to the grating surface. Curves for zero, first, and second orders are given, as well as the total energy reflected by the grating Σn.

Off-plane Resolution

$$R = \frac{2\tan\beta\sin\gamma}{B} \approx \frac{4\theta}{B}$$

At 2 degrees and 15" resolution
R=1800

Sub-Aperturing Improves
it Further

Biggest Problem is Focal Depth
(Starts at R~1200)

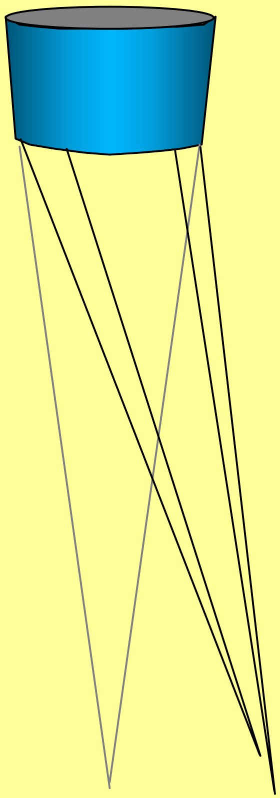

Solutions for Study:

Smaller Gratings
Curved Gratings
Add Chromatic Aberration
Adjust Telescope Segments

Internal Structure of Telescope

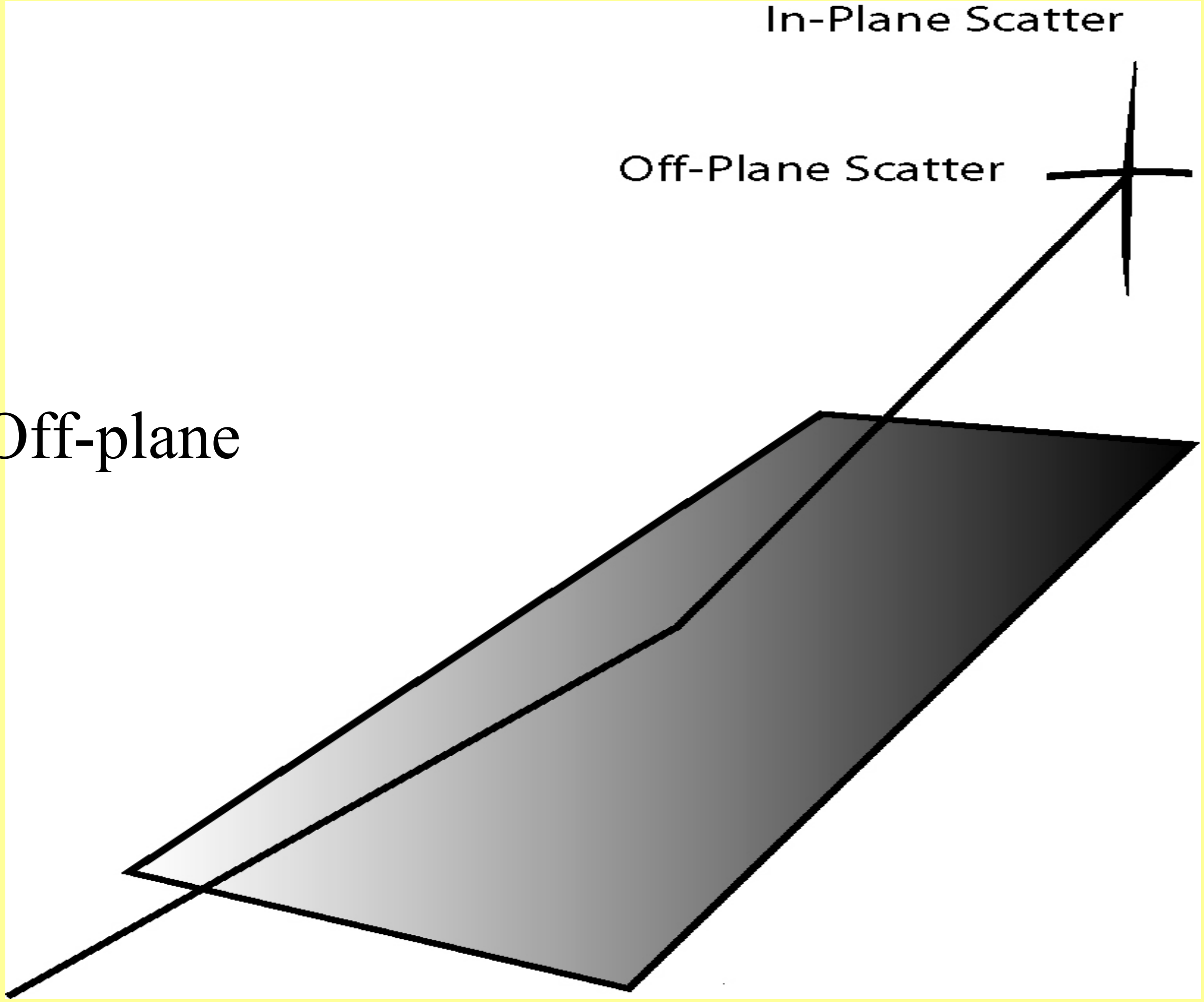

Blur Favors
Dispersion in Off-plane
Direction

ALL X-ray Telescopes Have This Internal Structure

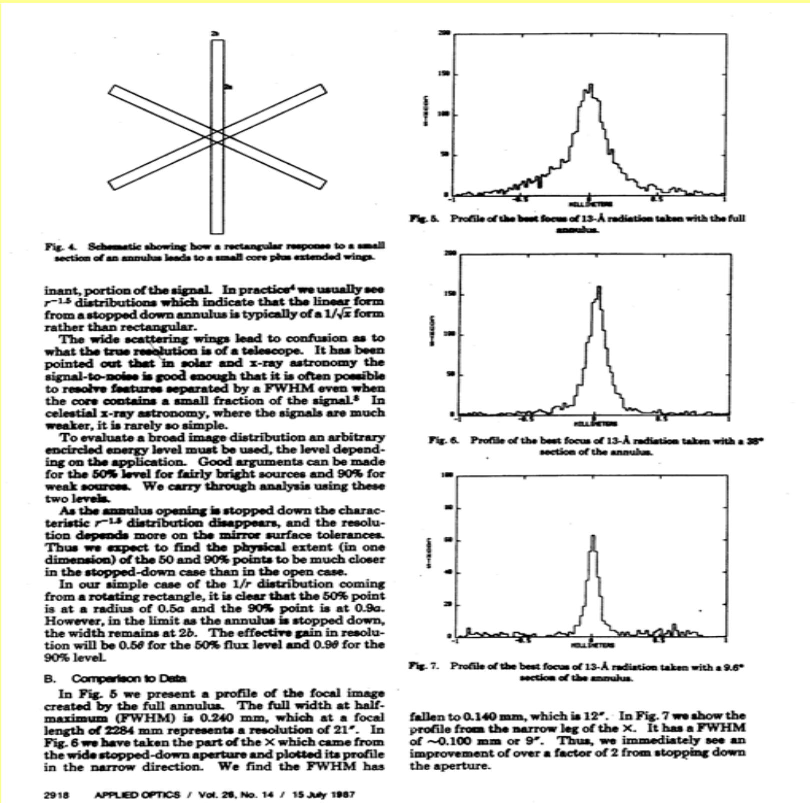

Fig. 4. Schematic showing how a rectangular response to a small section of an annulus leads to a small core plus extended wings.

inant, portion of the signal. In practice[4] we usually see $r^{-1.5}$ distributions which indicate that the linear form from a stopped down annulus is typically of a $1/\sqrt{x}$ form rather than rectangular.

The wide scattering wings lead to confusion as to what the true resolution is of a telescope. It has been pointed out that in solar and x-ray astronomy the signal-to-noise is good enough that it is often possible to resolve features separated by a FWHM even when the core contains a small fraction of the signal.[5] In celestial x-ray astronomy, where the signals are much weaker, it is rarely so simple.

To evaluate a broad image distribution an arbitrary encircled energy level must be used, the level depending on the application. Good arguments can be made for the 50% level for fairly bright sources and 90% for weak sources. We carry through analysis using these two levels.

As the annulus opening is stopped down the characteristic $r^{-1.5}$ distribution disappears, and the resolution depends more on the mirror surface tolerances. Thus we expect to find the physical extent (in one dimension) of the 50 and 90% points to be much closer in the stopped-down case than in the open case.

In our simple case of the $1/r$ distribution coming from a rotating rectangle, it is clear that the 50% point is at a radius of $0.5a$ and the 90% point is at $0.9a$. However, in the limit as the annulus is stopped down, the width remains at $2b$. The effective gain in resolution will be 0.5θ for the 50% flux level and 0.9θ for the 90% level.

B. Comparison to Data

In Fig. 5 we present a profile of the focal image created by the full annulus. The full width at half-maximum (FWHM) is 0.240 mm, which at a focal length of 2284 mm represents a resolution of 21″. In Fig. 6 we have taken the part of the × which came from the wide stopped-down aperture and plotted its profile in the narrow direction. We find the FWHM has fallen to 0.140 mm, which is 12″. In Fig. 7 we show the profile from the narrow leg of the ×. It has a FWHM of ~0.100 mm or 9″. Thus, we immediately see an improvement of over a factor of 2 from stopping down the aperture.

Fig. 5. Profile of the best focus of 13-Å radiation taken with the full annulus.

Fig. 6. Profile of the best focus of 13-Å radiation taken with a 38° section of the annulus.

Fig. 7. Profile of the best focus of 13-Å radiation taken with a 9.6° section of the annulus.

2918 APPLIED OPTICS / Vol. 26, No. 14 / 15 July 1987

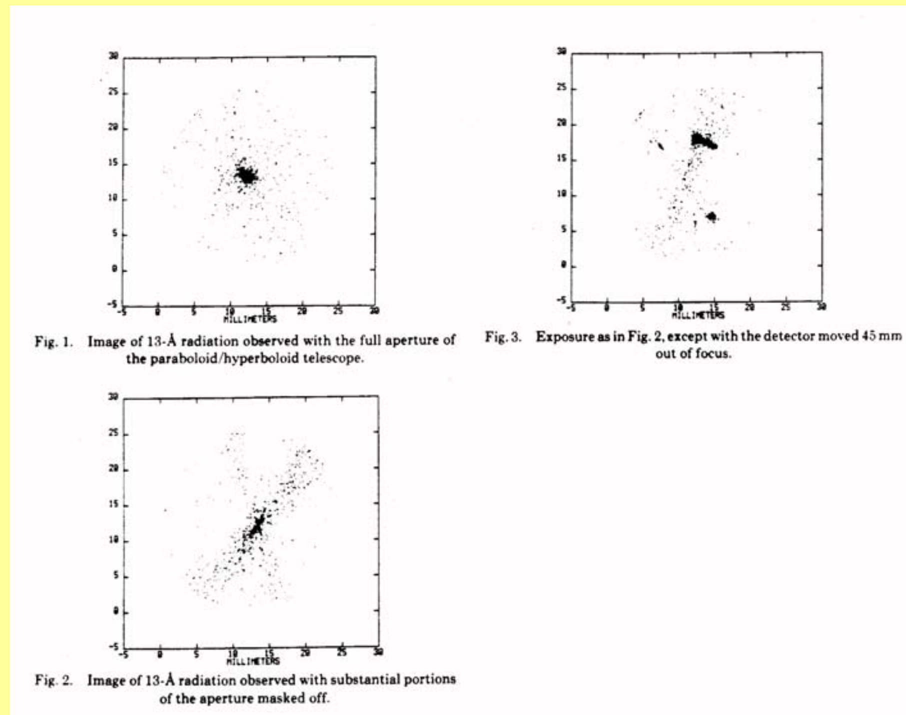

Fig. 1. Image of 13-Å radiation observed with the full aperture of the paraboloid/hyperboloid telescope.

Fig. 3. Exposure as in Fig. 2, except with the detector moved 45 mm out of focus.

Fig. 2. Image of 13-Å radiation observed with substantial portions of the aperture masked off.

Can Improve Performance

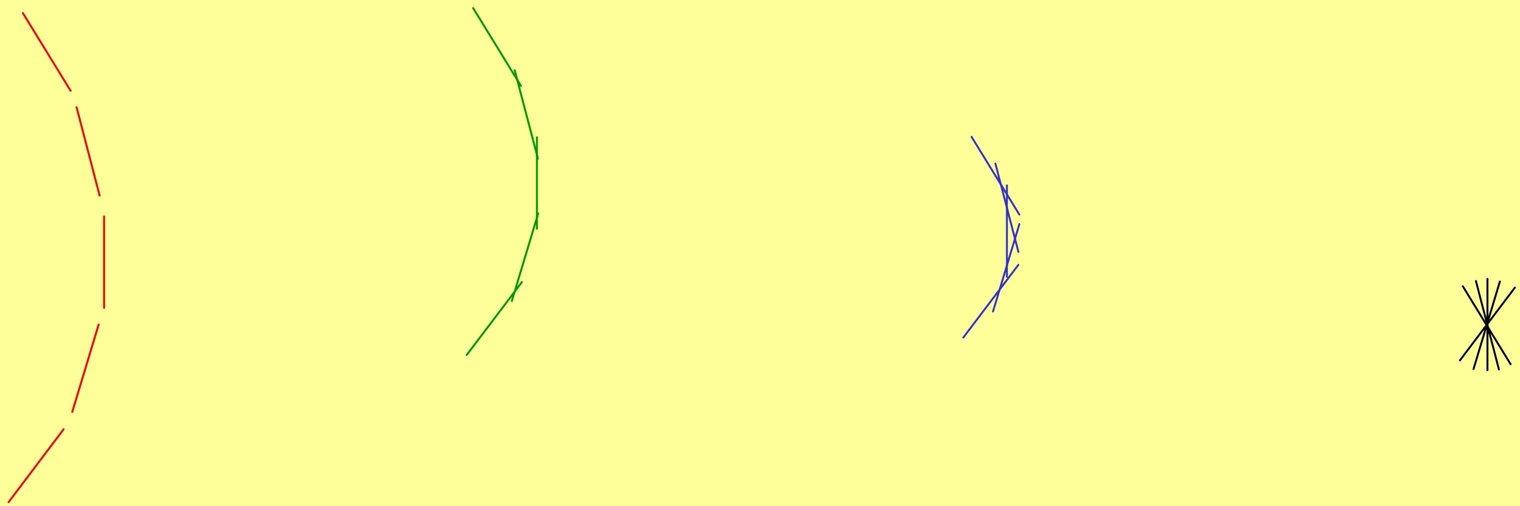

Raytracing – Arc of Diffraction

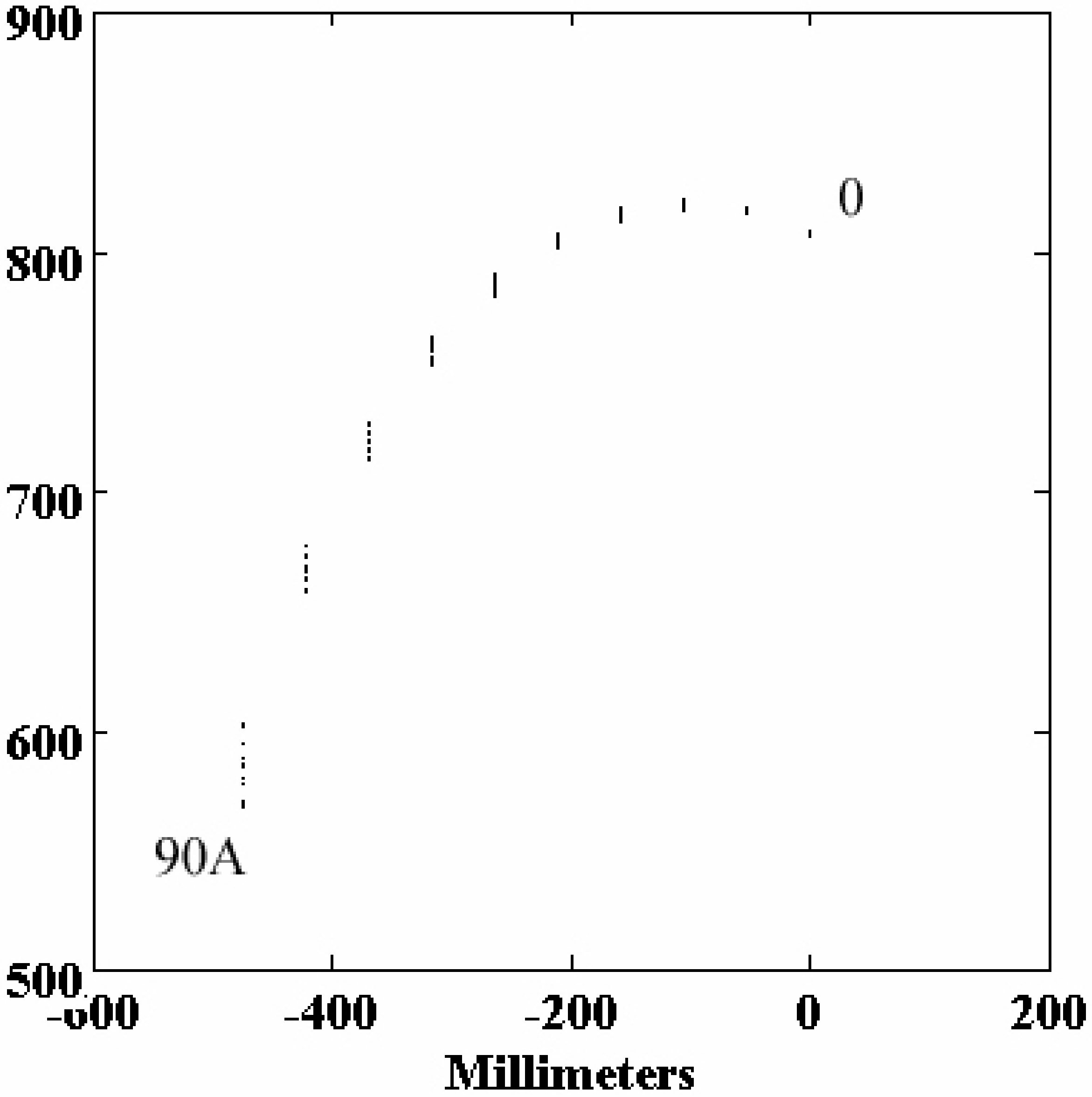

Raytrace – 35 & 35.028Å

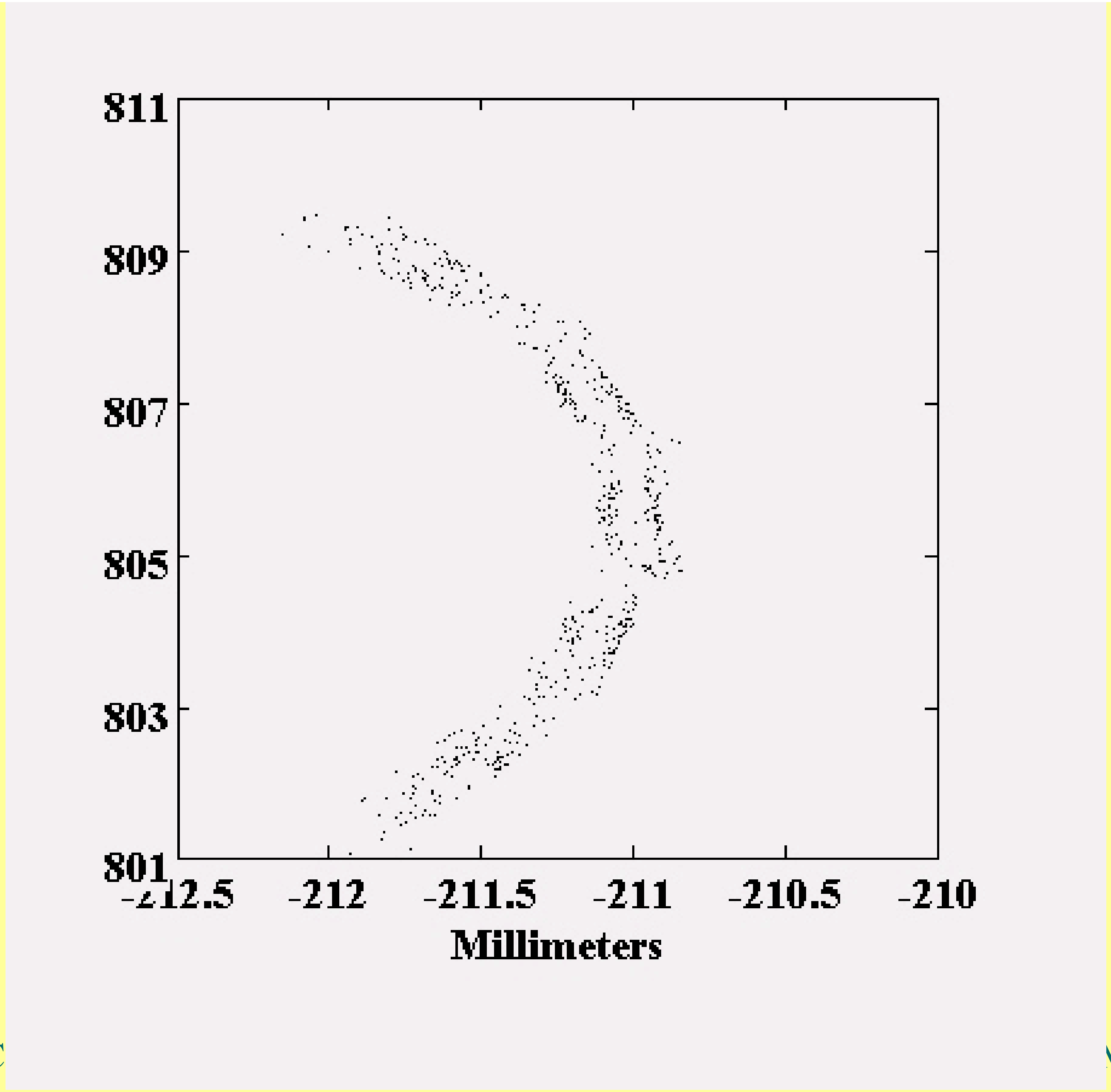

Raytracing of Wavelength Pairs
λ and λ+.028Å

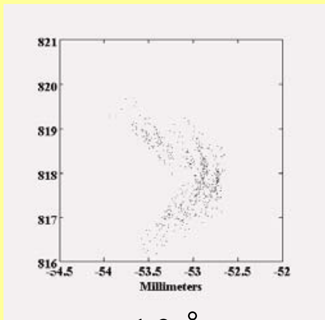

10Å

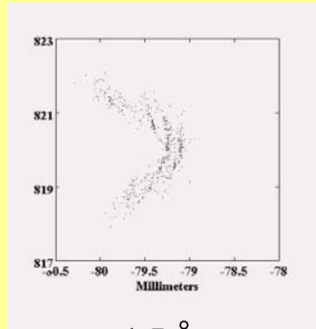

15Å

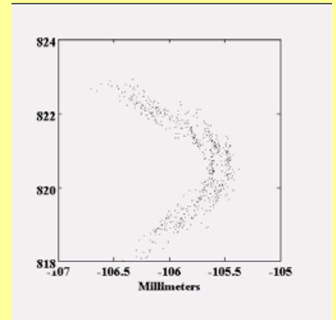

20Å

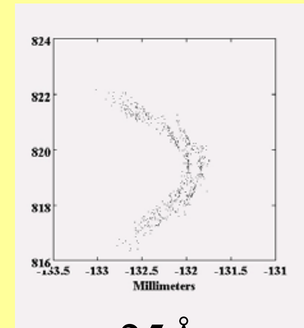

25Å

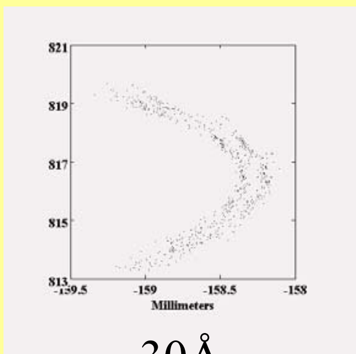

30Å

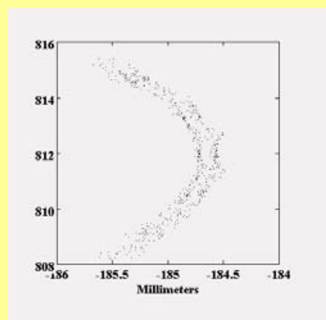

35Å

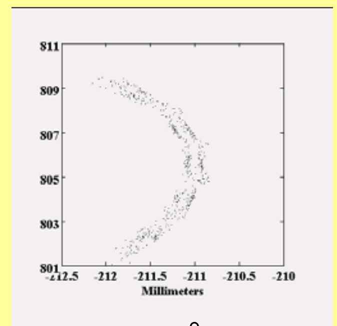

40Å

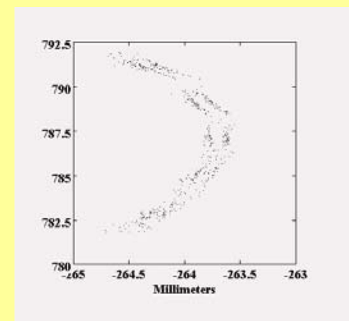

50Å

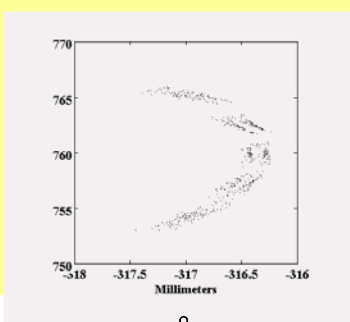

60Å

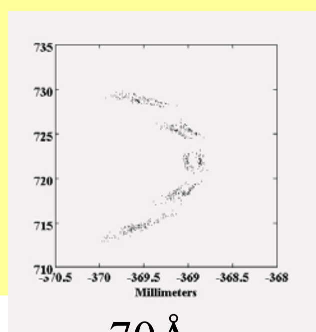

70Å

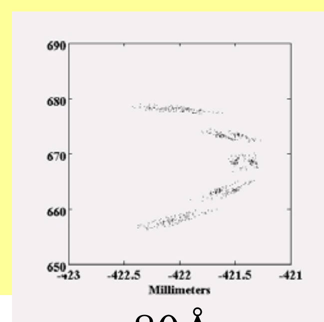

80Å

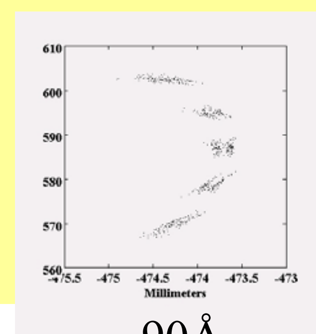

90Å

Resolution

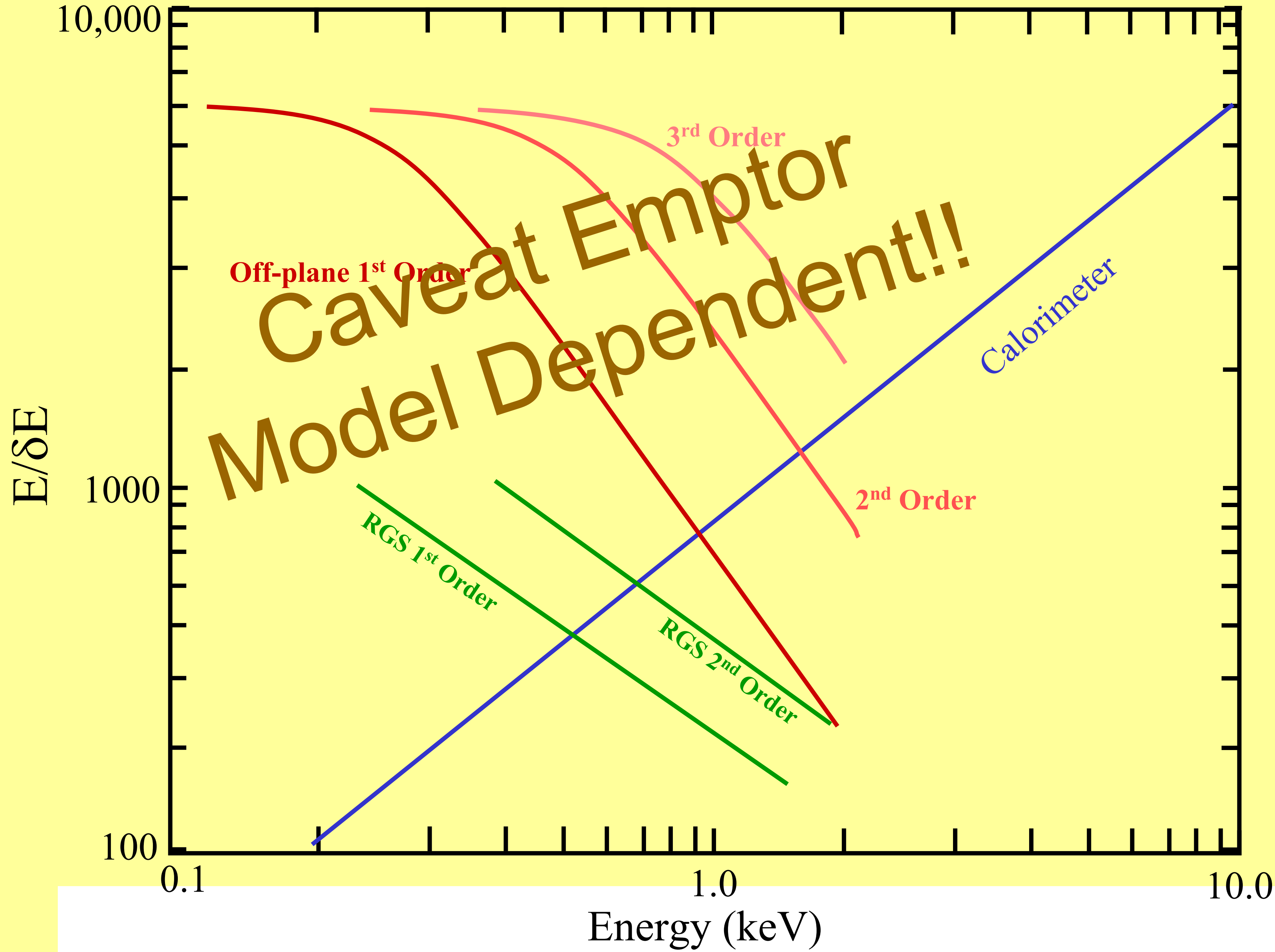

10,000
1000
100
E/δE
0.1
1.0
10.0
Energy (keV)
Off-plane 1st Order
3rd Order
2nd Order
RGS 1st Order
RGS 2nd Order
Calorimeter
Caveat Emptor
Model Dependent!!

Effective Area

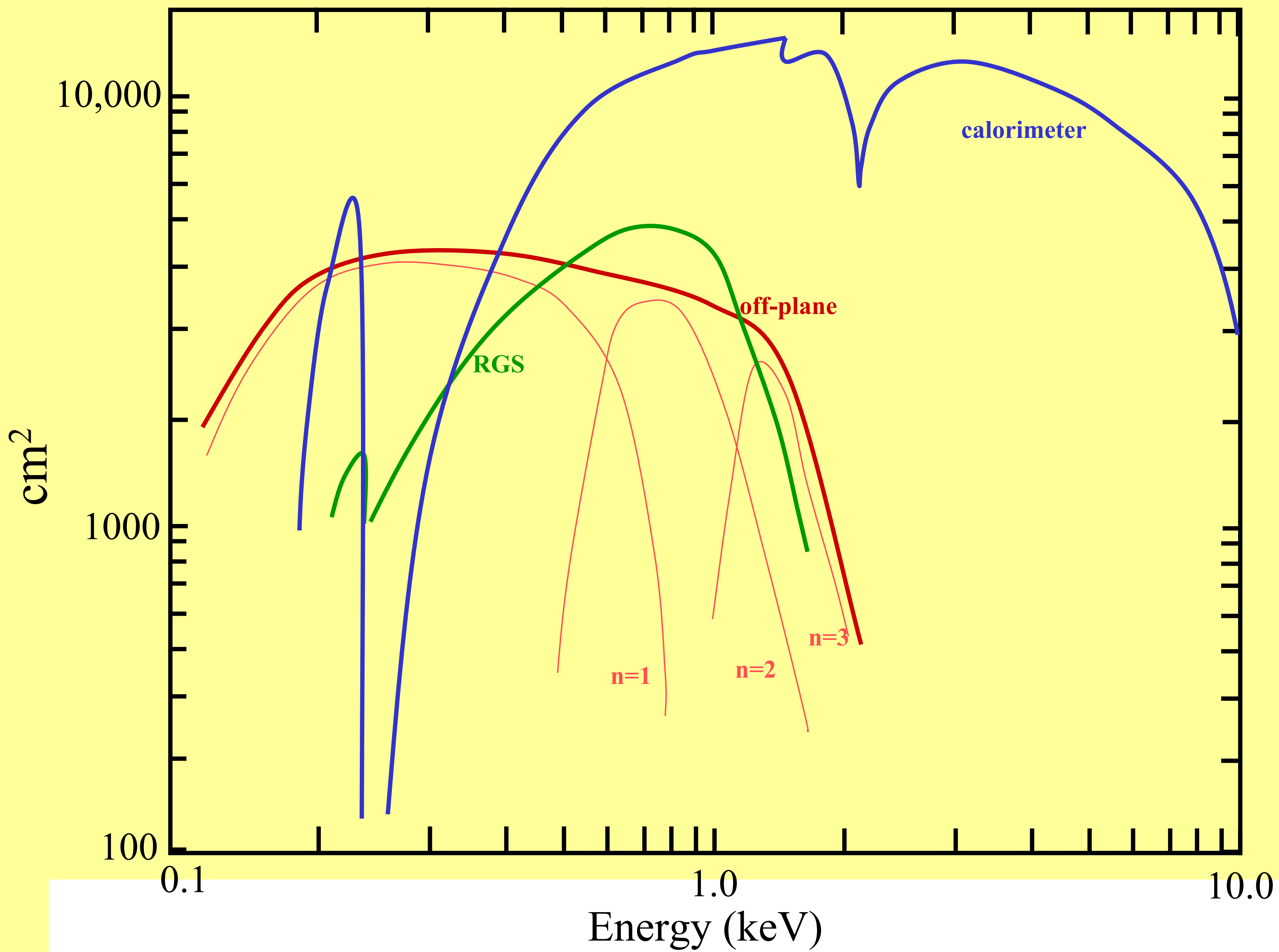

Holographic Gratings

Last year we reviewed approaches to fabricating high density gratings.

At Jobin-Yvon (outside Paris)
Create rulings using interference pattern in resist
Ion-Etch Master to Create Blaze

Radial Geometry – Type 4 Aberrated Beams?
Density: Up to 5800 g/mm Triangular (<35 deg blaze)

In UV holographic blazed gratings have *very* low scatter and good efficiency – same in x-ray?

Off-Plane Development Program

Six Month Evaluation	Completed November 2001
Build Test Master 58mm	November 2002
Evaluate in Lab	December 2002
Build Flight Master 128mm	June 2003
Replication Demonstration	May 2003

Goal: Achieve at least TRL 5 by mid-2004

Grating production issues

Direct Fabrication

- Identical gratings can be fabricated.
- Can utilize Si(111) crystal planes to form smooth, flat blazed grating facets on lightweight Si substrates thinned during fabrication.
- Thin substrates will require an arraying scheme that maintains grating flatness, not only reduction of twist.
- If off-plane geometry:
  - Combination of high ruling density (~150A facets) and large blaze angle may prove difficult to realize.
- If in-plane geometry:
  - Already fabricated and tested a single, uniform ruling density, directly fabricated grating.

Replication (using master)

- Extrapolating from XMM/Newton RGS experience, high fidelity grating replication (for 8000 parts) from a single master may require production of 7^{th} or 9^{th} generation replicas in a complex replication tree.
- If off-plane geometry:
  - mass constraints may be met with a more aggressive mass reduction in an arraying scheme similar to RGS on XMM/Newton.
  - Optical tolerances will apply to replica registration onto substrate and in-plane rotational positioning of replicas. (optical tolerances may also apply to ruling straightness)
- If in-plane geometry:
  - Mass constraints remain challenging; significant departures from XMM/Newton approach will be necessary to meet constraints.
  - Loose tolerances on replica registration on substrates.

Summary

Gratings are in Development

Two Viable Paths